HHS Public Access

Author manuscript

Acta Biomater. Author manuscript; available in PMC 2017 February 01.

Published in final edited form as:

Acta Biomater. 2016 February ; 31: 50–60. doi:10.1016/j.actbio.2015.11.043.

Inhibition of COX1/2 alters the host response and reduces ECM scaffold mediated constructive tissue remodeling in a rodent model of skeletal muscle injury

Christopher L. Dearth[#1,2,3,#], **Peter F. Slivka**[#1], **Scott A. Stewart**[1], **Timothy J. Keane**[1,4], **Justin K. Tay**[1], **Ricardo Londono**[1,5], **Qingnian Goh**[6], **Francis X. Pizza**[6], and **Stephen F. Badylak**[1,2,4]

[1] McGowan Institute for Regenerative Medicine, Pittsburgh, PA 15219

[2] Department of Surgery, University of Pittsburgh, Pittsburgh, PA 15219

[3] DoD-VA Extremity Trauma & Amputation Center of Excellence, Walter Reed National Military Medical Center, Bethesda, MD 20889

[4] Department of Bioengineering, University of Pittsburgh, Pittsburgh, PA 15213

[5] Medical Scientist Training Program, University of Pittsburgh, Pittsburgh, PA 15261

[6] Department of Kinesiology, The University of Toledo, Toledo, OH 43606

[#] These authors contributed equally to this work.

Abstract

Extracellular matrix (ECM) has been used as a biologic scaffold material to both reinforce the surgical repair of soft tissue and serve as an inductive template to promote a constructive tissue remodeling response. Success of such an approach is dependent on macrophage-mediated degradation and remodeling of the biologic scaffold. Macrophage phenotype during these processes is a predictive factor of the eventual remodeling outcome. ECM scaffolds have been shown to promote an anti-inflammatory or M2-like macrophage phenotype *in vitro* that includes secretion of downstream products of cycolooxygenases 1 and 2 (COX1/2). The present study investigated the effect of a common COX1/2 inhibitor (Aspirin) on macrophage phenotype and tissue remodeling in a rodent model of ECM scaffold treated skeletal muscle injury. Inhibition of COX1/2 reduced the constructive remodeling response by hindering myogenesis and collagen deposition in the defect area. The inhibited response was correlated with a reduction in M2-like macrophages in the defect area. The effects of Aspirin on macrophage phenotype were corroborated using an established *in vitro* macrophage model which showed a reduction in both ECM induced prostaglandin secretion and expression of a marker of M2-like macrophages (CD206). These results raise questions regarding the common peri-surgical administration of

[#] Corresponding Author: Christopher L. Dearth, PhD, Senior Scientist, DoD-VA Extremity Trauma & Amputation Center of Excellence, Walter Reed National Military Medical Center, Bethesda, MD 20889, Tel: 301-319-2461, Fax: 412-624-5256, Christopher.L.Dearth.civ@mail.mil.

COX1/2 inhibitors when biologic scaffold materials are used to facilitate muscle repair/regeneration.

Graphical Abstract

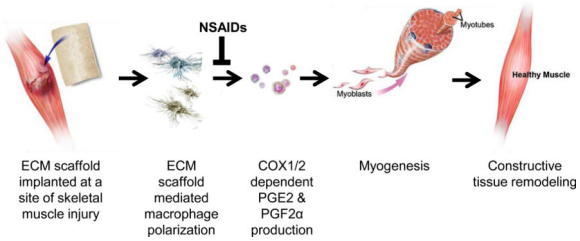

1. Introduction

Biologic scaffolds composed of ECM have been widely used to reinforce the surgical repair of soft tissue defects and to mediate an improved or constructive remodeling outcome[1-6]. While the clinical applications of ECM scaffolds are quite diverse and constantly expanding, skeletal muscle reinforcement (e.g. hernia repair and volumetric muscle loss) remains one of the most prevalent clinical applications for these materials[2,3]. When placed at the site of injury, ECM scaffolds orchestrate a complex host response that includes the recruitment of endogenous cells, such as immune cells and stem/progenitor cells[7-10]. Degradation of the scaffold by infiltrating host cells releases a variety of bioactive molecules that drive neovascularization, innervation, and site appropriate tissue formation[11-14].

One important feature of ECM scaffolds during the remodeling process is their ability to modulate macrophage phenotype. ECM scaffolds from a variety of source tissues promote an M2-like bias ($CD163^{high}$, $CD206^{high}$, $CD86^{low}$, $CCR7^{low}$) in the infiltrating macrophage population[9,15]. This bias has been shown to be a determinant factor in a favorable tissue remodeling outcome[9,10]. While a complete characterization of macrophage phenotype during tissue remodeling has yet to be completed, several studies have begun to describe this M2-like phenotype[16,17].

Recently, an enzymatically digested ECM scaffold derived from porcine urinary bladder (urinary bladder matrix, UBM) was found to up-regulate prostaglandin-E2 (PGE2) and prostaglandin-F2α (PGF2α) secretion in macrophages as part of a larger change in the overall macrophage phenotype[18]. Prostaglandin production requires the cyclooxygenase enzymes COX1 (constitutively expressed) and COX2 (inducibly expressed)[19]. Several studies have shown that COX2 knockout macrophages do not become fully M2 polarized and assume an M1-like phenotype[20,21]. Moreover, while prostaglandins can enhance the inflammatory response and pain states, these molecules are important mediators of tissue repair particularly in the context of skeletal muscle[22-24]. Collectively, these observations imply a potentially important role for COX1/2 in ECM-mediated macrophage polarization, and ultimately in constructive remodeling of ECM scaffolds.

COX1/2 inhibitors such as nonsteroidal anti-inflammatory drugs (NSAIDs) are typically available over-the-counter and taken for pain relief, and are routinely administered post-

surgically, primarily for anti-inflammatory and analgesic purposes[25]. While COX1/2 inhibitors are important in pain management, they have also been shown to delay or diminish the healing process, including macrophage accumulation; leading some to question their clinical use in treating musculotendinous injuries [26-34]. The effect of administration of NSAIDs upon ECM scaffold remodeling is unknown. The purpose of the present study was to determine the effect of a common NSAID, Aspirin, on the constructive remodeling response mediated by an ECM scaffold (UBM) in a rat skeletal muscle injury model.

2. Materials and Methods

2.1 Overview of Experimental Design

An established rodent skeletal muscle injury model was used to evaluate the effect of the COX1/2 inhibitor, Aspirin, on the ECM scaffold mediated constructive remodeling response[35,36]. Briefly, three days prior to the surgical procedure, animals were randomly assigned to either the Aspirin treated (3 mg/mL Aspirin in drinking water) or control (vehicle) group. Bilateral 1.5 cm × 1.5 cm partial thickness defects were created in the abdominal musculature. A size-matched pre-cast UBM hydrogel and an overlying 2 × 2 cm single layer sheet of UBM was then placed in the muscle defect area. The remodeling response was evaluated following 3, 7, 14, and 35 days by quantitative histomorphologic metrics[37,38], including characterization of macrophage phenotype and neo tissue deposition.

Established *in vitro* models were subsequently used to further interrogate the effect of Aspirin on ECM scaffold mediated macrophage function / polarization and myogenesis. *In vitro* macrophage function and polarization was characterized by quantification of secreted factor production and cell surface marker expression, respectively. *In vitro* myogenesis was characterized by an objective image analysis approach which quantified key events of myogenesis, such as the formation of multinucleated myotubes and myonuclear accretion.

2.2 Reagents

All chemicals were purchased from Sigma-Aldrich (St. Louis, MO) unless otherwise specified. All cell culture supplies were purchased from Life Technologies (Carlsbad, CA) unless otherwise specified. All chemicals used in this study were molecular biology grade or cell culture grade where appropriate.

2.3 Urinary Bladder Matrix Preparation

Porcine urinary bladders from market weight animals were acquired from Tissue Source, LLC. (Lafayette, Indiana). The ECM prepared from this tissue and referred to as UBM was prepared as previously described[39]. Briefly, the tunica serosa, tunica muscularis externa, tunica submucosa, and tunica muscularis mucosa were mechanically removed. The luminal urothelial cells of the tunica mucosa were dissociated by washing with sterile water. The remaining tissue consisting of basement membrane and subjacent tunica propria of the tunica mucosa was decellularized by agitation in 0.1% peracetic acid with 4% ethanol for 2 hours at 300 rpm. The tissue was then extensively rinsed with phosphate-buffered saline (PBS) and sterile water. The UBM was then lyophilized into a dry sheet and used as such, where appropriate, or milled into particulates using a Wiley Mill with a #60 mesh screen[40].

2.4 Pepsin Mediated ECM Solubilization and Hydrogel Formation

UBM was enzymatically digested with pepsin as described[41]. Milled UBM particulates (10 mg/mL) and pepsin (1 mg/mL) were placed in 0.01 M HCl (pH 2.0, sterile filtered) and stirred at room temperature for 48 hours. The thick slurry was then neutralized to a pH of 7.4 in sterile 1X PBS (137 mM NaCl, 2.7 mM KCl, 12 mM Phosphate, Fisher Scientific, Waltham, MA) to inactivate the pepsin. A solution of pepsin (1 mg/mL) in 0.01M HCl, treated in the same fashion as the UBM sample, served as the control condition for all experiments. All steps were conducted under sterile conditions with sterile filtered solutions. To form hydrogels, the neutralized slurry was placed in a 1.4 × 1.4 × 0.5 cm plastic mold and incubated at 37 °C for 30 minutes. For cell culture experiments, the solid UBM hydrogel was broken into smaller pieces with vigorous agitation and pipetting. The subsequent slurry was then added directly to cells. For animal studies, the UBM hydrogel was removed from the mold and placed directly into the defect site.

2.5 In-Vivo Study

Female Sprague Dawley rats (350 – 400 g at implantation) were purchased from Harlan Laboratories. Rats were housed on a 12 hour light-dark cycle and fed standard laboratory chow and water ad libitum. All animal procedures were approved by The University of Pittsburgh Institutional Animal Care and Use Committee (IACUC).

Animals were randomly assigned to either the Aspirin treated or control (vehicle) group. Three days prior to surgery, animals in the Aspirin group had their drinking water supplemented with 3 mg/mL Aspirin which was continued throughout the experimental time course. Consumption of water and animal weight was tracked daily throughout the duration of the study. Salicylates in whole blood were determined using the Salicylates Detection Kit from Neogen according to the manufacturer's instructions. Analysis of circulating salicylate content revealed a total salicylate concentration of 64 μg/mL in the NSAID treated group and no detectable salicylate content in the untreated group (Supplemental Figure 1).

2.6 Surgical Procedure

Anesthesia was induced with 2.5-4% isoflurane inhalant anesthetic and maintained at 0.5-3% throughout the procedure. The ventral abdomen was prepared for aseptic survival surgery by clipping the fur over the entire abdominal region, and cleaning the operative area with three alternating scrubs of providone-iodine surgical scrub and 70% isopropyl alcohol solutions. A final preparation of 70% isopropyl alcohol was applied and allowed to dry, followed by an application of DuraPrep™, which was allowed to dry before applying and placing sterile surgical drape(s) over the entire field.

A 4 cm midline skin incision was made and the skin was bluntly reflected to expose the abdominal muscle. Bilateral 1.5 cm × 1.5 cm partial thickness paramedian defects approximately 1 cm apart were created in the abdominal muscle. The defects were filled with size-matched pre-cast UBM hydrogels placed in the defect area (n=4 implants / group / time point). To prevent migration of the hydrogel, a 2 × 2 cm single layer sheet of UBM was placed over the hydrogel and secured with 4-0 PROLENE™ interrupted sutures placed at the corners. The skin was closed with a continuous (inner) 4-0 VICRYL™ suture. Upon

completion of the surgical procedure, the inhalant anesthetic was discontinued, and the animal was allowed to recover from anesthesia. The animal was given access to food and water ad libitum. Daily observations of each animal were made. The abdominal region of each animal was examined to assess both the condition of the wound line and subcutaneous tissues (e.g., dehiscence, seromas and/or hematomas).

2.7 Test Article Harvest

Euthanasia was administered by CO_2 inhalation and subsequent cervical dislocation, which was performed in accordance with the American Veterinary Medical Association (AVMA) Guidelines on Euthanasia. Following euthanasia, the skin was gently dissected, reflected, and photographs were taken of each defect *in situ*. After completion of the initial examination, the entire body wall that includes the test article was explanted *en bloc*. The specimen was then cut in half and each half immersed in 10% Neutral Buffered Formalin (NBF) for histologic analysis. A total of four test articles were collected and analyzed per treatment group per time point.

2.8 Immunolabeling and Quantification

CD206 and CD86—Cellular expression of markers of macrophage phenotype (CD206 and CD86) was determined by immunolabeling using previously described methods[9,8,15]. Briefly, paraffin embedded sections were washed with xylene and rehydrated slowly with an ethanol gradient. Antigen retrieval was accomplished by heating the sections to 95 °C in 0.01 M citrate buffer (pH = 6) for 25 min. Tissue sections were washed in Tris-Buffered Saline Tween-20 (TBST) and incubated in blocking buffer consisting of 2% horse serum albumin, 1% BSA, 0.05% Tween-20, and 0.05% Triton X-100 in TBS for 1 hour. For M1/M2 phenotype analysis, the primary antibodies, mouse anti-rat CD68 (pan-macrophage marker, 1:100 AbD Serotec, Raleigh, NC), goat anti-rat CD206 (M2 marker, 1:100 Santa Cruz, Dallas, TX), and rabbit anti-rat CD86 (M1 marker, 1:250, Abcam, Cambridge, England) were diluted in blocking buffer, added to the sections and incubated overnight at 4 °C in a humidified chamber. After primary labeling, tissue sections were washed extensively in PBS and species appropriate secondary antibodies (donkey anti-rabbit Alexa-Fluor 488 (1:300), donkey anti-mouse Alex-Fluor 594(1:300), donkey anti-goat PerCP Cy5.5 (1:300), Life Technologies, Carlsbad, CA)) were added and incubated for 1 hour at room temperature in a humidified chamber. Tissue sections were further washed with TBST and imaged by a blinded observer at 40X magnification using a Nikon Eclipse E600 microscope (Chiyoda, Tokyo) with CRi Nuance FX multispectral imaging system (Cambridge, MA). Four slides per treatment condition per time point were used for histological analysis. Four representative images of each colabeled tissue section were collected. The number of CD68+CD206+ (M2-like macrophages) and CD68+CD86+ (M1-like macrophages) cells per field of view (40x magnification) were quantified using a custom Cell Profiler pipeline[42].

Fast and Slow Myosin Heavy Chain—Myosin heavy chain positive cells in the defect area were determined by immunolabeling for fast and slow myosin heavy chain as previously described[14,43,44]. Briefly, slides were deparaffinized before epitope retrieval in 0.1 mM EDTA at 95 °C for 25 min followed by 0.1% trypsin/0.1% calcium chloride (w/v) at 37 °C for 10 min. Peroxidase activity in tissue sections was quenched by incubation in

0.3% (v/v) hydrogen peroxide solution in TBS for 10 min. Sections were then blocked with 2% horse serum, 1% BSA in TBS for 30 min. Sections were then immunolabeled for mouse anti-slow myosin heavy chain (1:1000, clone NOQ7.5.4D, M8421, SigmaAldrich) for 40 min and subsequently rinsed in TBS. Sections were incubated in biotinylated goat anti-mouse IgG secondary antibody (1:200, Vector) for 1 h at room temperature and rinsed in TBS. Sections were then stained in Vectastain ABC reagent (Vectastain Elite ABC Kit, Vector) for 30 min and developed with a diaminobenzadine substrate (ImmPact DAB, Vector). Sections were incubated in blocking solution for 10 min before incubation in alkaline phosphatase conjugated mouse anti-fast myosin heavy chain (1:200, clone MY-32, A4335, Sigma) for 1 hour. Color was developed by staining with alkaline phosphatase (Red Alkaline Phosphatase Kit, SK-5100, Vector), dehydrated, and mounted for imaging by blinded observers. To quantify the effect of Aspirin on ECM scaffold induced myogenesis, the myogenic index (total cross sectional area of myosin heavy chain positive cells as a function of the total defect area) was quantified on four slides at the 35 day timepoint. Specifically, mosaic images spanning the entire defect were obtained using a Zeiss Axio-Observer Z.1 microscope (Oberkochen, Germany), and each myosin heavy chain positive cell border was traced and the area quantified with ImageJ software. A blinded observer distinguished the location of the defect border from the intact native tissue and identified myogenesis by the presence of centrally located nuclei within cells that were also positive for myosin heavy chain. The MHC+ area at the earlier time points was not determined as a previous study showed that no myogenesis with UBM is observed before 35 days[38].

Picrosirius Red Staining and Imaging—The area of collagen fibers as a function of their color hue was quantified from four tissue sections stained with picrosirius red and imaged with circularly polarized light microscopy at 20X magnification. Four representative images of each stained tissue section were collected. The color hue corresponds to relative fiber thickness from thin green fibers to increasingly thick yellow, orange, and red fibers[37,45,46]. A custom Matlab (The Mathworks, Natick, MA) script transformed each image from the RGB to the HSV color model, separated each color component as a function of hue (red 2–9 and 230–256, orange 10–38, yellow 39–51, green 52–128), applied a threshold to remove noise from an average of a global threshold using Otsu's method (intensity value of 50/256), and expressed the collagen content for each color component as a percentage of the area of each image.

2.9 Macrophage Cell Culture

THP-1 human monocytes were obtained from the American Tissue Culture Collection (ATCC, Manassas, VA) and maintained in RPMI, 10% FBS, 1% penicillin/streptomycin, 2 mM L-glutamine, and 1 mM sodium pyruvate in a humidified atmosphere at 37 °C with 5% CO2. For experiments, 500,000 THP-1 cells/mL were plated with 320 nM phorbol 12-myristate 13-acetate (PMA) for 24 hours to induce differentiation into macrophages. Adherent macrophages were washed in PBS and placed in fresh media, followed by a 24 hour incubation to acquiesce. Resting THP1 cells after differentiation has been shown to provide a macrophage-like cell with similar behavior to primary human peripheral blood mononuclear cells[47].

Rat bone marrow mononuclear cells were matured to macrophages as previously described[48]. Briefly, bone marrow cells were flushed from leg bones of female Sprague Dawley rats, triturated in isolation media (DMEM high glucose media with 2% Penicillin-Streptomycin) and centrifuged. The cell pellet was resuspended in red blood cell (RBC) lysis buffer (155mM NH4Cl, 10mM KHCO3, 0.9%EDTA in distilled water) and incubated for 15 minutes on ice. Cell debris was removed by centrifugation and the cell pellet was resuspended in macrophage maturation media (DMEM high glucose, 10% heat inactivated FBS, 20% L929 fibroblast conditioned media, 0.5 mM MEM non-essential amino acids, 2 mM L-glutamine, 10 mM Hepes pH 7.4, 1% penicillin/streptomycin, 0.12% 50 mM 2-mercaptoethanol). Cells were seeded at a density of 1 million/mL in 6 well plates and incubated at 37 °C/5% CO2. Media was changed every 2-3 days for 7 days. Matured bone marrow derived macrophages (BMDMs) were treated with 1 mL of StemPro® Accutase® (Invitrogen), incubated at 37 °C for 10 minutes, and detached with gentle pipetting. The cell suspension was collected and centrifuged for 5 minutes at 1400 rpm. The cell pellet was resuspended in macrophage culture media (DMEM high glucose, 10% heat inactivated FBS, 0.5 mM MEM non-essential amino acids, 2 mM L-glutamine, 10 mM Hepes pH 7.4, 1% pennicillin/streptomycin, 0.12% 50mM 2-mercaptoethanol) and plated at a density of 500,000/mL. Cells were allowed to recover overnight before treatment.

Primary microglia from rats were obtained from postnatal day 3 rat pup brains as previously described[49]. Whole brains from postnatal day 3 Sprague Dawley rat pups (Charles River) were harvested and minced after removal of the brain stem, olfactory bulbs, and meninges. Tissue was digested for 15 minutes in 0.25% trypsin/EDTA at 37 °C. Brain tissues were triturated with a fire polished glass pipet in the presence of 1 mg/mL DNase I and 10% FBS. The suspension was centrifuged, diluted in culture media (DMEM/F12, 10%FBS, 2mM L-glutamine, 1% penicillin/streptomycin), and grown to confluence at 37 °C/5% CO2. Culture media was replaced every 2-3 days. At day 11-12 *in vitro*, enriched microglia were obtained by mechanical agitation (orbital shaker, 150 rpm, 37 C) for 2 hours. The media was collected after the shake-off step and centrifuged (1400 rpm for 5 minutes). The cell pellet was resuspended in culture media (RPMI 1640, 10% FBS, 1mM L-glutamine , 1mM sodium pyruvate , 50μM beta-mercaptoethanol, 1% penicillin and streptomycin) and cells were plated at a density of 500,000/mL. Microglia were allowed to recover for 24 hours prior to treatment.

2.10 Secreted Factor Analysis

Once cells were prepared as described above, aspirin (200 μM, where appropriate) was added for 1 hour. Subsequently, UBM hydrogel (0.5 mg/mL) or pepsin control buffer (0.05 mg/mL) was added and cells were allowed to incubate for 24-72 hours. After incubation, cells were pelleted by centrifugation (700×g, 5 minutes, 4 °C), and the culture supernatants were carefully removed. Supernatants were stored at −80 °C until the time of assay. Secreted factor concentrations in the culture supernatants were determined using commercially available ELISA kits (PGE2, PGF2α (ENZO Life Sciences) and IL-1RA (R&D Systems)) according to the manufacturer's instructions. Three independent replicates with two samples per replicate were performed for each experiment.

2.11 SDS PAGE and Western Blotting

At the specified time points, cells were washed extensively with 1X PBS and lysis buffer (50 mM Tris, 20 mM NaCl, 1% Triton X-100) was added. Cells were mechanically removed from the culture dish, transferred to centrifuge tubes and incubated on ice for 10 minutes. Lysates were spun down at 14000 rpm for 20 minutes at 4°C to remove any debris. The clarified lysate was stored at −80°C. Lysates were diluted 1:1 in 2X Laemmli Sample Buffer (Bio-Rad, Hercules, CA) and boiled at 95 °C for 5 minutes. Samples were then resolved on 9% SDS-PAGE gels (National Diagnostics) and transferred to polyvinyldifluoride (PVDF, Millipore) membranes. Membranes were blocked with 1:1 Odyssey Blocking Buffer:1XPBS (Licor) overnight at 4°C. Blocked membranes were immunoblotted with either rabbit anti-human COX2 (1:5,000, Abcam), goat anti-human CD206 (1:3,000, Santa-Cruz), rabbit anti-human CD86 (1:5,000, Abcam), or mouse anti-human β-Actin (1:5,000, Abcam) in blocking buffer for 1 hour at room temperature with agitation. Membranes were extensively washed with TBST before the appropriate secondary antibodies (1:10,000, donkey anti-goat IR Dye 680, donkey-anti rabbit IR Dye 680, donkey anti-mouse IR Dye 800, Licor) in imaging buffer (1:1 Odyssey Blocking Buffer, 0.02% SDS in TBST) were added for 30 minutes with agitation. After extensive washing in TBST, membranes were imaged using the Licor Odyssey system. Densitometry was performed using ImageJ. Four independent replicates were performed for the COX2 experiment and three were performed for CD206 and CD86 experiment.

2.12 In Vitro Myogenesis

C2C12 murine myoblasts were obtained from ATCC and grown in complete media (DMEM, 10% FBS, 1% penicillin/streptomycin) at 37 °C/5% CO2 according to the ATCC recommendations. Myoblasts were seeded at a density of 5,000 cells/cm^2 in 24 well plates and allowed proliferate to ~90% confluence. Cells were then washed in 1XPBS and incubated in differentiation media (DMEM, 2% horse Serum, 1% penicillin/streptomycin) for 24 hours. Cells were washed in 1XPBS and placed in basal media (DMEM, 1% penicillin/streptomycin). A transwell insert (Corning) containing 100,000 differentiated THP1 cells (as described in section 2.9) in 200 μL of complete THP1 cell media was placed in each well. UBM hydrogel (0.5 mg/mL, final concentration) was then added to the THP1 transwell insert only. Where appropriate, aspirin (200 μM) was added to the co-culture system first (i.e., ~5 minutes before the UBM hydrogel). Pepsin control buffer (0.05 mg/mL) and non-treated cells served as the controls. The co-culture was incubated for 48 hours. At the conclusion of the experimental duration the transwell inserts were removed and the C2C12 cells were washed in 1XPBS, fixed with 4% PFA for 15 minutes, permeabilized with 0.05% Triton X-100, treated with blocking buffer, and then immunolabeled with anti-sarcomeric myosin heavy chain (MHC) (1:20; clone MF20; Developmental Studies Hybridoma Bank) overnight at 4 °C. Cells were then incubated with Alexa-Fluor 488 secondary antibody (1:400, Invitrogen) and mounted with Fluoromount-G™ containing 4',6-Diamidino-2-phenylindole (DAPI; SouthernBiotech). A standardized image capture system and quantitative analysis of *in vitro* myogenesis was performed as previously described[50]. Briefly, custom macro functions (Image Pro 7; Media Cybernetics Inc.) were used to objectively quantify several important myogenesis parameters (e.g., the number of nuclei,

myotubes, and nuclei within a myotube). Myotubes were operationally defined as MHC+ cells with 2 or more nuclei and an area greater than 200 μm^2. The fusion index, which reflects myotube formation and myonuclear accretion, was calculated by expressing the number of nuclei within myotubes as a percentage of total nuclei. Three independent replicates were performed for each experiment.

2.13 Statistical Analysis

Where appropriate, a one-way or two-way analysis of variance (ANOVA) was performed to determine significant differences with Tukey post hoc testing ($p<0.05$). Data and error bars are reported as mean + standard deviation unless otherwise specified.

3. Results

The purpose of the present study was to determine the effect of the COX1/2 inhibitor, Aspirin, on the ECM mediated constructive remodeling response, including macrophage phenotype and tissue deposition, in a rat model of skeletal muscle injury. Aspirin administration reduced myogenesis and collagen deposition in the remodeling area and was associated with a reduction in CD206 expressing M2-like macrophages and an increase in CD86 expressing M1-like macrophages. The effect of Aspirin (200 μM) on macrophage phenotype was further corroborated using an established *in vitro* model which showed decreased secreted factor production (PGE2, PGF2α) and M2-like macrophage cell surface marker expression (CD206). The circulating salicylate concentration measured in vivo was approximately 355 μM. The 0.8 fold difference between these concentrations is reasonably similar and allows for comparison of *in vitro* and *in vivo* data sets.

3.1 The effect of Aspirin on ECM scaffold-mediated tissue remodeling

To quantify differences in tissue remodeling with Aspirin administration, the area of newly formed collagen and MHC+ cells within the defect borders were quantified using established metrics[37,44]. Picrosirius red staining of the defect area and imaging with polarized light microscopy showed a gradual increase in the abundance of collagen (5% to 25%) over the experimental time course in non-treated animals (Figure 1B). Administration of Aspirin altered the UBM-mediated remodeling response at the 35 day time point as shown by a 24% reduction in collagen deposition. ECM scaffold mediated *de novo* myogenesis was quantified by determining the myogenic index (Figure 2A). At 35 days post implantation, a 4 fold reduction in myogenesis was observed in the Aspirin treated animals compared to non-treated controls (Figure 2B). Collectively, these data suggest that Aspirin administration influences the UBM mediated constructive remodeling response by reducing both collagen content and myogenesis in the defect area.

3.2 The effect of NSAIDS on macrophage phenotype in vivo

To determine if Aspirin administration altered ECM scaffold mediated macrophage phenotype, $CD206^+CD68^+$ (M2-like) and $CD86^+CD68^+$ (M1-like) macrophages were immunolabeled and quantified using an automated cell profiler analysis pipeline (Figure 3)[15]. Aspirin treatment altered the phenotype of accumulated macrophages as shown by a reduction in the M2:M1 ratio (main effect for treatment) (Figure 3). Specifically, Aspirin

elicited both a reduction in M2 ($CD206^+$) and an increase in M1 ($CD86^+$) macrophages when compared with non-Aspirin treated animals throughout the experimental time course (Supplemental Figure 2). These data suggest that Aspirin alters the typical macrophage phenotype response mediated by ECM scaffolds *in vivo* based upon both reduced M2 marker expression and increased M1 marker expression.

3.3 UBM Mediates COX2 expression and prostaglandin secretion in vitro

To determine if Aspirin inhibited UBM-mediated COX2 expression or secretion of COX1/2 dependent small molecules, THP1 macrophage-like cells were treated with either UBM or UBM and Aspirin for 4, 8, and 24 hours. Western blots of cell lysates (Figure 4A) showed a steady increase in COX2 expression over the time course reaching a 1.2 fold maximum increase at 24 hours (Figure 4B). Aspirin did not cause any changes in COX2 expression. To determine the effect of Aspirin on the downstream products of COX2, the PGE2 and PGF2α concentration in culture supernatants was measured at 48 hours (Figure 5A and 5B). Treatment with Aspirin reduced production of both PGE2 and PGF2α down to basal levels. Secretion of a non-COX1/2 dependent factor (IL-1RA) was also examined. Aspirin did not cause any significant drop in IL-1RA secretion suggesting that, at minimum, the dose of Aspirin used was not cytotoxic to the cells (Figure 5C). The concentration of TNFα and IL-1β in the culture supernatants was also quantified over a 72 hour time course (Supplemental Figure 3). Minimal concentrations of TNFα or IL-1β were observed over the 72 hour timecourse suggesting that the UBM mediated production of prostaglandins is not merely a side effect of an acute pro-inflammatory response but rather a directed and controlled constructive remodeling response.

To validate the use of THP1 cells as a model system, PGE2 expression was examined in primary rat bone marrow derived macrophages and brain derived microglia. Treatment of primary cells with UBM for 48 hours mediated similar increases in PGE2 compared to THP1 cells (Supplemental Figure 4). Inhibition of COX1/2 with Aspirin reduced PGE2 production to baseline levels in all three cell types. Collectively, these data suggest that UBM activation of PGE2 production is not restricted to the THP1 cell line, and inhibition of COX1/2 is also observed in primary cells.

3.4 The effect of Aspirin on macrophage phenotype

To test the effects of UBM and COX1/2 inhibition on macrophage phenotype, THP1 cells were treated with UBM and changes in their CD206 and CD86 expression profile were determined by western blotting (Figure 6A and 6C). Treatment with UBM increased CD206 expression (0.4 fold – 0.57 fold above control) at 4, 8, and 24 hours post treatment (Figure 6B). Increases in CD206 expression were concurrent with a drop in CD86 expression that reached a maximum reduction (0.2 fold) at 24 hours (Figure 6D). Treatment with aspirin did not alter CD206 expression at the early time points. However, at 24 hours a significant reduction (91%) in CD206 expression was observed with Aspirin treatment. Likewise, treatment with Aspirin caused a steady increase in CD86 expression reaching a maximum 0.15 fold increase at 24 hours that was significantly higher than UBM treatment alone (0.2 fold decrease). Collectively, these data suggest that Aspirin treatment inhibits the UBM

initiated M2 bias in macrophages by decreasing CD206 expression and increasing CD86 expression.

3.5 Aspirin treatment reduces myogenesis in vitro

A dynamic interplay between macrophages and skeletal muscle cells is an important component of the skeletal muscle repair/regeneration process following injury. Recently, the secreted products from ECM scaffold induced M2-like macrophages were found to stimulate myogenesis of skeletal muscle progenitor cells *in vitro*[51]. To more accurately replicate the kinetics of this interaction between an ECM scaffold, macrophages, and skeletal muscle cells over time; a co-culture system was utilized in which THP1 cells were placed in the same culture well as C2C12 myoblasts, via a transwell insert. UBM (0.5 mg/mL) with or without Aspirin (200 μM) was added to the THP1 cell insert only and the system was incubated for 48 hours. Addition of UBM caused robust increases in fusion index (43%), (Figure 7). These data indicate that UBM treatment causes macrophages to secrete factors that facilitate myoblast differentiation and fusion into myotubes. Co-administration of aspirin with UBM reduced the fusion index down to control levels (Figure 7). Collectively, these data suggest that a COX1/2 inhibitor impairs the ability of macrophages to secrete pro-myogenic factors in response to UBM.

4. Discussion

ECM scaffolds facilitate constructive and site appropriate tissue remodeling when implanted into a variety of tissue sites including skeletal muscle [14,43,52-54]. However, occasionally these materials fail to induce or only partially induce a constructive tissue remodeling response with some patients showing robust functional improvement and others showing little improvement along with a marked inflammatory response[55-60]. One potential source of these divergent results may lie in the pre- and post-operative regimen prescribed for these patients (e.g., NSAID administration, physical therapy, etc.). The results presented herein suggest that Aspirin can negatively impact the constructive remodeling events elicited by ECM scaffolds, in terms of bona fide myogenesis and macrophage polarization, both of which are critical for effective repair/regeneration of skeletal muscle tissue.

Previous studies utilizing knockout animals or small molecule inhibitors have described a vital role of COX2 activity in endogenous skeletal muscle repair / regeneration [26,27,29-34,61-64,63,65]. While this detrimental effect of NSAIDs on endogenous skeletal muscle repair is well described, little is known about the effect of NSAIDs on ECM scaffold mediated skeletal muscle repair/constructive remodeling. The current study demonstrated that administration of Aspirin reduced ECM scaffold mediated myogenesis both *in vitro* and *in vivo*. Direct study of myotube formation in the THP1/C2C12 co culture system corroborates the *in vivo* reduction in myogenesis (79%) with a similar reduction in fusion index (92%). Collectively, the data presented herein suggest that COX1/2 activity, namely PGE2 and PGF2α, is a critical component of the ECM scaffold mediated tissue remodeling response.

Macrophages and their acquired phenotype / function, are critical components of the wound healing response[9,10,66]. A well-orchestrated phenotypic response beginning with an M1-like

phenotype during the early (i.e. debridment) part of healing and transitioning to a prolonged M2-like phenotype during the repair phase has been well described[66,67]. A strong M2-like bias in the macrophage population is consistently observed when an ECM scaffold is utilized which precedes an improved remodeling outcome[9]. The results presented herein confirm these reports as UBM mediated an increase in M2 marker expression (CD206) and a decrease in M1 marker expression (CD86) both *in vitro* and *in vivo*. Inhibition of COX2 reversed these trends driving a stronger M1 macrophage response. These findings support several recent studies which have shown that COX2 and its downstream products are an important component in the development of an M2-like phenotype[20]. Knockout of the COX2 gene in rodents prevents macrophages from progressing along the M2 spectrum[21]. The results of the present study must be interpreted with caution as the reliance on two markers to describe macrophage phenotype is an oversimplification of a complex phenomenon. However, a number of studies utilizing ECM scaffolds to treat similar (skeletal muscle) and unrelated (esophageal, TMJ) injury models have consistently shown a bias towards CD206 and away from CD86, validating the use of these markers and the results presented herein[15,37,55].

As several studies on musculotendinous and skeletal injury have shown that NSAIDs delay but do not prevent the maximum healing response[68-70], additional work is needed to determine if the effects reported herein irreparably reduce the regenerative response or if the response is simply delayed. Specifically, collagen deposition could be associated with a scar tissue response and/or the formation of site appropriate tissue (i.e., constructive remodeling). Thus, studies with longer follow up durations are needed to completely assess the full kinetic effect of NSAIDs after ECM scaffold implantation. Furthermore, the time scale of NSAID administration warrants further investigation. While some studies have shown beneficial effects of NSAIDs for musculoskeletal injuries when administered acutely to manage the symptomatology of inflammation[71,72], others have shown no effects or inhibitory effects over similar time scales[73,74]. Given the confounding nature of these results, future studies are needed to evaluate the effects of the duration of NSAID administration on ECM scaffold mediated constructive remodeling. Lastly, the present *in vivo* study was limited by the use of immunolabeling to measure the effects of NSAIDs on myogenesis. While there was a 4-fold reduction in myogenic index, it is unknown whether this change translates to differences in functional outcomes.

The present study investigated the influence of COX2 in mediating several important events in the complex host response to an ECM scaffold material. The COX1/2 inhibitor, Aspirin, was found to mitigate the ECM scaffold-mediated constructive remodeling response both in an *in vitro* co-culture system and an *in vivo* rat model of skeletal muscle injury. While further studies are needed to more completely characterize this response, the results presented herein provide data to substantiate the possibility that the use of NSAIDs may significantly alter tissue remodeling outcomes when a biomaterial is used in a regenerative medicine / tissue engineering application. Thus, the decision to prescribe NSAIDs to manage the symptomatology of inflammation either pre- or post-ECM scaffold implantation should be approached with care.

Supplementary Material

Refer to Web version on PubMed Central for supplementary material.

Acknowledgements

This material is based upon work supported by the National Institute of Health under Grant Number 1R03EB018889-01A1 (to C.L.D. & P.F.S) and Grant Number 5T32EB001026-09 (R.L.), National Science Foundation Graduate Research Fellowship under Grant Number DGE-1247842 (to T.J.K.), and the DoD-VA Extremity Trauma & Amputation Center of Excellence (Public Law 110-417, National Defense Authorization Act 2009, Section 723).

Disclaimer: Any opinion, findings, and conclusions or recommendations expressed in this material are those of the authors(s) and do not necessarily reflect the official views, policy, or position of the National Science Foundation, Department of the Army, Department of Defense, nor the U.S. Government.

References

1. Badylak SF. The extracellular matrix as a biologic scaffold material. Biomaterials. 2007; 28(25): 3587–93. [PubMed: 17524477]
2. Hope WW, Griner D, Adams A, Hooks WB, Clancy TV. Use and indications of human acellular dermis in ventral hernia repair at a community hospital. Plast Surg Int. 2012; 2012:918345. [PubMed: 23094147]
3. Kissane NA, Itani KM. A decade of ventral incisional hernia repairs with biologic acellular dermal matrix: what have we learned? Plast Reconstr Surg. 2012; 130(5 Suppl 2):194S–202S. [PubMed: 23096971]
4. Derwin KA, Badylak SF, Steinmann SP, Iannotti JP. Extracellular matrix scaffold devices for rotator cuff repair. J Shoulder Elbow Surg. 2010; 19(3):467–76. [PubMed: 20189415]
5. Mofid MM, Meininger MS, Lacey MS. Veritas(R) bovine pericardium for immediate breast reconstruction: a xenograft alternative to acellular dermal matrix products. Eur J Plast Surg. 2012; 35(10):717–722. [PubMed: 23002328]
6. Ricchetti ET, Aurora A, Iannotti JP, Derwin KA. Scaffold devices for rotator cuff repair. J Shoulder Elbow Surg. 2012; 21(2):251–65. [PubMed: 22244069]
7. Beattie AJ, Gilbert TW, Guyot JP, Yates AJ, Badylak SF. Chemoattraction of progenitor cells by remodeling extracellular matrix scaffolds. Tissue Eng Part A. 2009; 15(5):1119–25. [PubMed: 18837648]
8. Vorotnikova E, McIntosh D, Dewilde A, Zhang J, Reing JE, Zhang L, Cordero K, Bedelbaeva K, Gourevitch D, Heber-Katz E. Extracellular matrix-derived products modulate endothelial and progenitor cell migration and proliferation in vitro and stimulate regenerative healing in vivo. Matrix Biol. 2010; 29(8):690–700. others. [PubMed: 20797438]
9. Brown BN, Londono R, Tottey S, Zhang L, Kukla KA, Wolf MT, Daly KA, Reing JE, Badylak SF. Macrophage phenotype as a predictor of constructive remodeling following the implantation of biologically derived surgical mesh materials. Acta Biomater. 2012; 8(3):978–87. [PubMed: 22166681]
10. Brown BN, Valentin JE, Stewart-Akers AM, McCabe GP, Badylak SF. Macrophage phenotype and remodeling outcomes in response to biologic scaffolds with and without a cellular component. Biomaterials. 2009; 30(8):1482–91. [PubMed: 19121538]
11. Agrawal V, Brown BN, Beattie AJ, Gilbert TW, Badylak SF. Evidence of innervation following extracellular matrix scaffold-mediated remodelling of muscular tissues. J Tissue Eng Regen Med. 2009; 3(8):590–600. [PubMed: 19701935]
12. Brown BN, Badylak SF. Expanded applications, shifting paradigms and an improved understanding of host-biomaterial interactions. Acta Biomater. 2012; 9(2):4948–55. [PubMed: 23099303]
13. Turner NJ, Badylak JS, Weber DJ, Badylak SF. Biologic scaffold remodeling in a dog model of complex musculoskeletal injury. J Surg Res. 2011; 176(2):490–502. [PubMed: 22341350]

14. Turner NJ, Yates AJ Jr. Weber DJ, Qureshi IR, Stolz DB, Gilbert TW, Badylak SF. Xenogeneic extracellular matrix as an inductive scaffold for regeneration of a functioning musculotendinous junction. Tissue Eng Part A. 2010; 16(11):3309–17. [PubMed: 20528669]
15. Keane TJ, Londono R, Carey RM, Carruthers CA, Reing JE, Dearth CL, D'Amore A, Medberry CJ, Badylak SF. Preparation and characterization of a biologic scaffold from esophageal mucosa. Biomaterials. 2013; 34(28):6729–37. [PubMed: 23777917]
16. Franz S, Allenstein F, Kajahn J, Forstreuter I, Hintze V, Moller S, Simon JC. Artificial extracellular matrices composed of collagen I and high-sulfated hyaluronan promote phenotypic and functional modulation of human pro-inflammatory M1 macrophages. Acta Biomater. 2013; 9(3):5621–9. [PubMed: 23168224]
17. Freytes DO, Kang JW, Marcos-Campos I, Vunjak-Novakovic G. Macrophages modulate the viability and growth of human mesenchymal stem cells. J Cell Biochem. 2013; 114(1):220–9. [PubMed: 22903635]
18. Slivka PF, Dearth CL, Keane TJ, Meng FW, Medberry C, Riggio RT, Reing JE, Badylak SF. Fractionation of an ECM Hydrogel into Structural and Soluble Components Reveals Distinctive Roles in Regulating Macrophage Behavior. Biomaterials Science. 2014; 2:1521–1534.
19. Flower RJ. The development of COX2 inhibitors. Nat Rev Drug Discov. 2003; 2(3):179–91. [PubMed: 12612644]
20. Na YR, Yoon YN, Son DI, Seok SH. Cyclooxygenase-2 inhibition blocks M2 macrophage differentiation and suppresses metastasis in murine breast cancer model. PLoS One. 2013; 8(5):e63451. [PubMed: 23667623]
21. Nakanishi Y, Nakatsuji M, Seno H, Ishizu S, Akitake-Kawano R, Kanda K, Ueo T, Komekado H, Kawada M, Minami M. COX-2 inhibition alters the phenotype of tumor-associated macrophages from M2 to M1 in ApcMin/+ mouse polyps. Carcinogenesis. 2011; 32(9):1333–9. others. [PubMed: 21730361]
22. Rakoff-Nahoum S, Medzhitov R. Prostaglandin-secreting cells: a portable first aid kit for tissue repair. J Clin Invest. 2007; 117(1):83–6. [PubMed: 17200710]
23. Van Ly D, Burgess JK, Brock TG, Lee TH, Black JL, Oliver BG. Prostaglandins but not leukotrienes alter extracellular matrix protein deposition and cytokine release in primary human airway smooth muscle cells and fibroblasts. Am J Physiol Lung Cell Mol Physiol. 2012; 303(3):L239–50. [PubMed: 22637153]
24. Lane NE. Pain management in osteoarthritis: the role of COX-2 inhibitors. J Rheumatol Suppl. 1997; 49:20–4. [PubMed: 9249647]
25. Xian CJ, Zhou XF. Treating skeletal pain: limitations of conventional anti-inflammatory drugs, and anti-neurotrophic factor as a possible alternative. Nat Clin Pract Rheumatol. 2009; 5(2):92–8. [PubMed: 19182815]
26. Bondesen BA, Mills ST, Kegley KM, Pavlath GK. The COX-2 pathway is essential during early stages of skeletal muscle regeneration. Am J Physiol Cell Physiol. 2004; 287(2):C475–83. [PubMed: 15084473]
27. Bondesen BA, Mills ST, Pavlath GK. The COX-2 pathway regulates growth of atrophied muscle via multiple mechanisms. Am J Physiol Cell Physiol. 2006; 290(6):C1651–9. [PubMed: 16467402]
28. Horsley V, Pavlath GK. Prostaglandin F2(alpha) stimulates growth of skeletal muscle cells via an NFATC2-dependent pathway. J Cell Biol. 2003; 161(1):111–8. [PubMed: 12695501]
29. Shen W, Li Y, Tang Y, Cummins J, Huard J. NS-398, a cyclooxygenase-2-specific inhibitor, delays skeletal muscle healing by decreasing regeneration and promoting fibrosis. Am J Pathol. 2005; 167(4):1105–17. [PubMed: 16192645]
30. Shen W, Li Y, Zhu J, Schwendener R, Huard J. Interaction between macrophages, TGF-beta1, and the COX-2 pathway during the inflammatory phase of skeletal muscle healing after injury. J Cell Physiol. 2008; 214(2):405–12. [PubMed: 17657727]
31. Shen W, Prisk V, Li Y, Foster W, Huard J. Inhibited skeletal muscle healing in cyclooxygenase-2 gene-deficient mice: the role of PGE2 and PGF2alpha. J Appl Physiol (1985). 2006; 101(4):1215–21. [PubMed: 16778000]

32. Mendias CL, Tatsumi R, Allen RE. Role of cyclooxygenase-1 and -2 in satellite cell proliferation, differentiation, and fusion. Muscle Nerve. 2004; 30(4):497–500. [PubMed: 15372441]
33. Mikkelsen UR, Helmark IC, Kjaer M, Langberg H. Prostaglandin synthesis can be inhibited locally by infusion of NSAIDS through microdialysis catheters in human skeletal muscle. J Appl Physiol (1985). 2008; 104(2):534–7. [PubMed: 18079272]
34. Mikkelsen UR, Langberg H, Helmark IC, Skovgaard D, Andersen LL, Kjaer M, Mackey AL. Local NSAID infusion inhibits satellite cell proliferation in human skeletal muscle after eccentric exercise. J Appl Physiol (1985). 2009; 107(5):1600–11. [PubMed: 19713429]
35. Valentin JE, Badylak JS, McCabe GP, Badylak SF. Extracellular matrix bioscaffolds for orthopaedic applications. A comparative histologic study. J Bone Joint Surg Am. 2006; 88(12): 2673–86. [PubMed: 17142418]
36. Sicari B, Turner N, Badylak SF. An in vivo model system for evaluation of the host response to biomaterials. Methods Mol Biol. 2013; 1037:3–25. [PubMed: 24029927]
37. Wolf MT, Carruthers CA, Dearth CL, Crapo PM, Huber A, Burnsed OA, Londono R, Johnson SA, Daly KA, Stahl EC. Polypropylene surgical mesh coated with extracellular matrix mitigates the host foreign body response. J Biomed Mater Res A. 2013 others.
38. Wolf MT, Daly KA, Brennan-Pierce EP, Johnson SA, Carruthers CA, D'Amore A, Nagarkar SP, Velankar SS, Badylak SF. A hydrogel derived from decellularized dermal extracellular matrix. Biomaterials. 2012; 33(29):7028–38. [PubMed: 22789723]
39. Freytes DO, Tullius RS, Badylak SF. Effect of storage upon material properties of lyophilized porcine extracellular matrix derived from the urinary bladder. J Biomed Mater Res B Appl Biomater. 2006; 78(2):327–33. [PubMed: 16365866]
40. Gilbert TW, Stolz DB, Biancaniello F, Simmons-Byrd A, Badylak SF. Production and characterization of ECM powder: implications for tissue engineering applications. Biomaterials. 2005; 26(12):1431–5. [PubMed: 15482831]
41. Freytes DO, Martin J, Velankar SS, Lee AS, Badylak SF. Preparation and rheological characterization of a gel form of the porcine urinary bladder matrix. Biomaterials. 2008; 29(11): 1630–7. [PubMed: 18201760]
42. Carpenter AE, Jones TR, Lamprecht MR, Clarke C, Kang IH, Friman O, Guertin DA, Chang JH, Lindquist RA, Moffat J. CellProfiler: image analysis software for identifying and quantifying cell phenotypes. Genome Biol. 2006; 7(10):R100. others. [PubMed: 17076895]
43. Valentin JE, Turner NJ, Gilbert TW, Badylak SF. Functional skeletal muscle formation with a biologic scaffold. Biomaterials. 2010; 31(29):7475–84. [PubMed: 20638716]
44. Wolf MT, Daly KA, Reing JE, Badylak SF. Biologic scaffold composed of skeletal muscle extracellular matrix. Biomaterials. 2012; 33(10):2916–25. [PubMed: 22264525]
45. Cuttle L, Nataatmadja M, Fraser JF, Kempf M, Kimble RM, Hayes MT. Collagen in the scarless fetal skin wound: detection with picrosirius-polarization. Wound Repair Regen. 2005; 13(2):198–204. [PubMed: 15828945]
46. Nadkarni SK, Pierce MC, Park BH, de Boer JF, Whittaker P, Bouma BE, Bressner JE, Halpern E, Houser SL, Tearney GJ. Measurement of collagen and smooth muscle cell content in atherosclerotic plaques using polarization-sensitive optical coherence tomography. J Am Coll Cardiol. 2007; 49(13):1474–81. [PubMed: 17397678]
47. Daigneault M, Preston JA, Marriott HM, Whyte MK, Dockrell DH. The identification of markers of macrophage differentiation in PMA-stimulated THP-1 cells and monocyte-derived macrophages. PLoS One. 2010; 5(1):e8668. [PubMed: 20084270]
48. Boltz-Nitulescu G, Wiltschke C, Holzinger C, Fellinger A, Scheiner O, Gessl A, Forster O. Differentiation of rat bone marrow cells into macrophages under the influence of mouse L929 cell supernatant. J Leukoc Biol. 1987; 41(1):83–91. [PubMed: 3543182]
49. Shaked I, Tchoresh D, Gersner R, Meiri G, Mordechai S, Xiao X, Hart RP, Schwartz M. Protective autoimmunity: interferon-gamma enables microglia to remove glutamate without evoking inflammatory mediators. J Neurochem. 2005; 92(5):997–1009. [PubMed: 15715651]
50. Goh Q, Dearth CL, Corbett JT, Pierre P, Chadee DN, Pizza FX. Intercellular adhesion molecule-1 expression by skeletal muscle Cells Augments myogenesis. Exp Cell Res. 2014

51. Sicari BM, Dziki JL, Siu BF, Medberry CJ, Dearth CL, Badylak SF. The promotion of a constructive macrophage phenotype by solubilized extracellular matrix. Biomaterials. 2014; 35(30):8605–12. [PubMed: 25043569]
52. Badylak S, Kokini K, Tullius B, Simmons-Byrd A, Morff R. Morphologic study of small intestinal submucosa as a body wall repair device. J Surg Res. 2002; 103(2):190–202. [PubMed: 11922734]
53. Badylak S, Kokini K, Tullius B, Whitson B. Strength over time of a resorbable bioscaffold for body wall repair in a dog model. J Surg Res. 2001; 99(2):282–7. [PubMed: 11469898]
54. Daly KA, Wolf M, Johnson SA, Badylak SF. A rabbit model of peripheral compartment syndrome with associated rhabdomyolysis and a regenerative medicine approach for treatment. Tissue engineering Part C, Methods. 2011; 17(6):631–40. [PubMed: 21361746]
55. Sicari BM, Rubin JP, Dearth CL, Wolf MT, Ambrosio F, Boninger M, Turner NJ, Weber DJ, Simpson TW, Wyse A. An acellular biologic scaffold promotes skeletal muscle formation in mice and humans with volumetric muscle loss. Sci Transl Med. 2014; 6(234):234ra58. others.
56. Gupta A, Zahriya K, Mullens PL, Salmassi S, Keshishian A. Ventral herniorrhaphy: experience with two different biosynthetic mesh materials, Surgisis and Alloderm. Hernia. 2006; 10(5):419–25. [PubMed: 16924395]
57. Ansaloni L, Cambrini P, Catena F, Di Saverio S, Gagliardi S, Gazzotti F, Hodde JP, Metzger DW, D'Alessandro L, Pinna AD. Immune response to small intestinal submucosa (surgisis) implant in humans: preliminary observations. J Invest Surg. 2007; 20(4):237–41. [PubMed: 17710604]
58. Shah BC, Tiwari MM, Goede MR, Eichler MJ, Hollins RR, McBride CL, Thompson JS, Oleynikov D. Not all biologics are equal! Hernia. 2011; 15(2):165–71. [PubMed: 21188442]
59. Harth KC, Rosen MJ. Major complications associated with xenograft biologic mesh implantation in abdominal wall reconstruction. Surg Innov. 2009; 16(4):324–9. [PubMed: 20031943]
60. Harris HW. Clinical outcomes of biologic mesh: where do we stand? Surg Clin North Am. 2013; 93(5):1217–25. [PubMed: 24035084]
61. Deng B, Wehling-Henricks M, Villalta SA, Wang Y, Tidball JG. IL-10 triggers changes in macrophage phenotype that promote muscle growth and regeneration. J Immunol. 2012; 189(7): 3669–80. [PubMed: 22933625]
62. Kharraz Y, Guerra J, Mann CJ, Serrano AL, Munoz-Canoves P. Macrophage plasticity and the role of inflammation in skeletal muscle repair. Mediators Inflamm. 2013; 2013:491497. [PubMed: 23509419]
63. Mo C, Romero-Suarez S, Bonewald L, Johnson M, Brotto M. Prostaglandin E2: from clinical applications to its potential role in bone-muscle crosstalk and myogenic differentiation. Recent Pat Biotechnol. 2012; 6(3):223–9. [PubMed: 23092433]
64. Zhang L, Dong Y, Cheng J, Du J. Role of integrin-beta3 protein in macrophage polarization and regeneration of injured muscle. J Biol Chem. 2011; 287(9):6177–86. [PubMed: 22210777]
65. Brewer C, Waddell D. The Role of Prostaglandin F2Alpha in Skeletal Muscle Regeneration. Journal of Trainology. 2012; 1:45–52.
66. Tidball JG. Inflammatory processes in muscle injury and repair. Am J Physiol Regul Integr Comp Physiol. 2005; 288(2):R345–53. [PubMed: 15637171]
67. Tidball JG. Mechanisms of muscle injury, repair, and regeneration. Compr Physiol. 2011; 1(4): 2029–62. [PubMed: 23733696]
68. Almekinders LC, Baynes AJ, Bracey LW. An in vitro investigation into the effects of repetitive motion and nonsteroidal antiinflammatory medication on human tendon fibroblasts. Am J Sports Med. 1995; 23(1):119–23. [PubMed: 7726341]
69. Greene JM, Winickoff RN. Cost-conscious prescribing of nonsteroidal anti-inflammatory drugs for adults with arthritis. A review and suggestions. Arch Intern Med. 1992; 152(10):1995–2002. [PubMed: 1417372]
70. Kulick MI, Smith S, Hadler K. Oral ibuprofen: evaluation of its effect on peritendinous adhesions and the breaking strength of a tenorrhaphy. J Hand Surg Am. 1986; 11(1):110–20. [PubMed: 3511134]
71. Baldwin AC, Stevenson SW, Dudley GA. Nonsteroidal anti-inflammatory therapy after eccentric exercise in healthy older individuals. Journals of Gerontology Series a-Biological Sciences and Medical Sciences. 2001; 56(8):M510–M513.

72. van den Bekerom MP, Sjer A, Somford MP, Bulstra GH, Struijs PA, Kerkhoffs GM. Non-steroidal anti-inflammatory drugs (NSAIDs) for treating acute ankle sprains in adults: benefits outweigh adverse events. Knee Surg Sports Traumatol Athrosc. 2014

73. Slatyer MA, Hensley MJ, Lopert R. A randomized controlled trial of piroxicam in the management of acute ankle sprain in Australian Regular Army recruits. The Kapooka Ankle Sprain Study. Am J Sports Med. 1997; 25(4):544–53. [PubMed: 9240990]

74. Astrom M, Westlin N. No effect of piroxicam on achilles tendinopathy. A randomized study of 70 patients. Acta Orthop Scand. 1992; 63(6):631–4. [PubMed: 1471511]

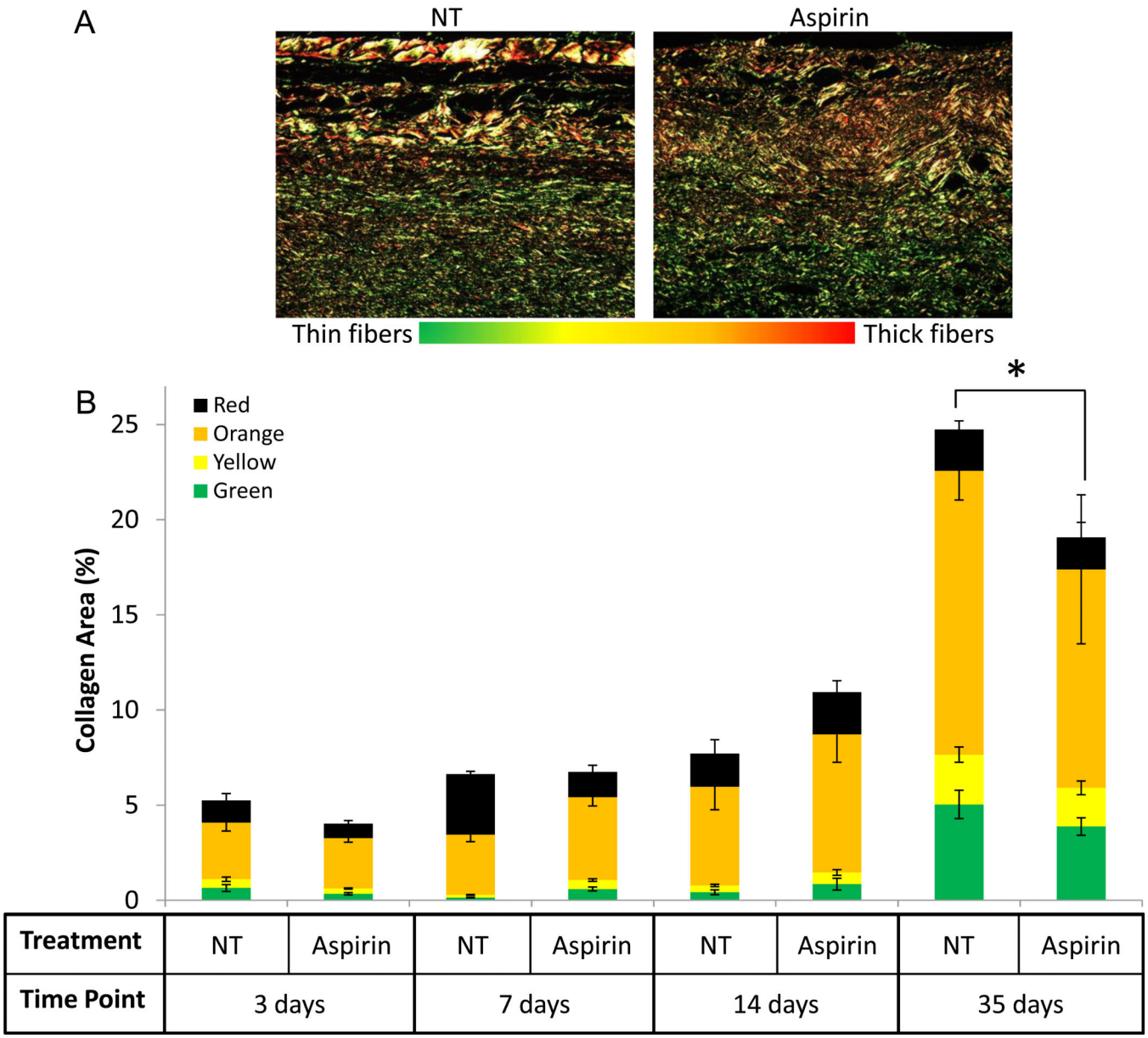

Figure 1.

The effect of aspirin administration on UBM stimulated collagen deposition *in vivo*. Tissue sections from the specified time points were stained with picrosirius red and imaged using polarized light microscopy. (A) Representative images of tissue sections from untreated and aspirin treated animals 35 days post operatively are shown. The color hue of the fibers represents the relative collagen thicknesses (in order of thinnest to thickest): green, yellow, orange, and red. (B) The total area and proportion of collagen thickness in non-treated (NT) and Aspirin treated (ASPIRIN) animals after 3, 7, 14, and 35 days was assessed utilizing an automated MatLab script. Significant decreases in total collagen deposition are shown ($p<0.05$).

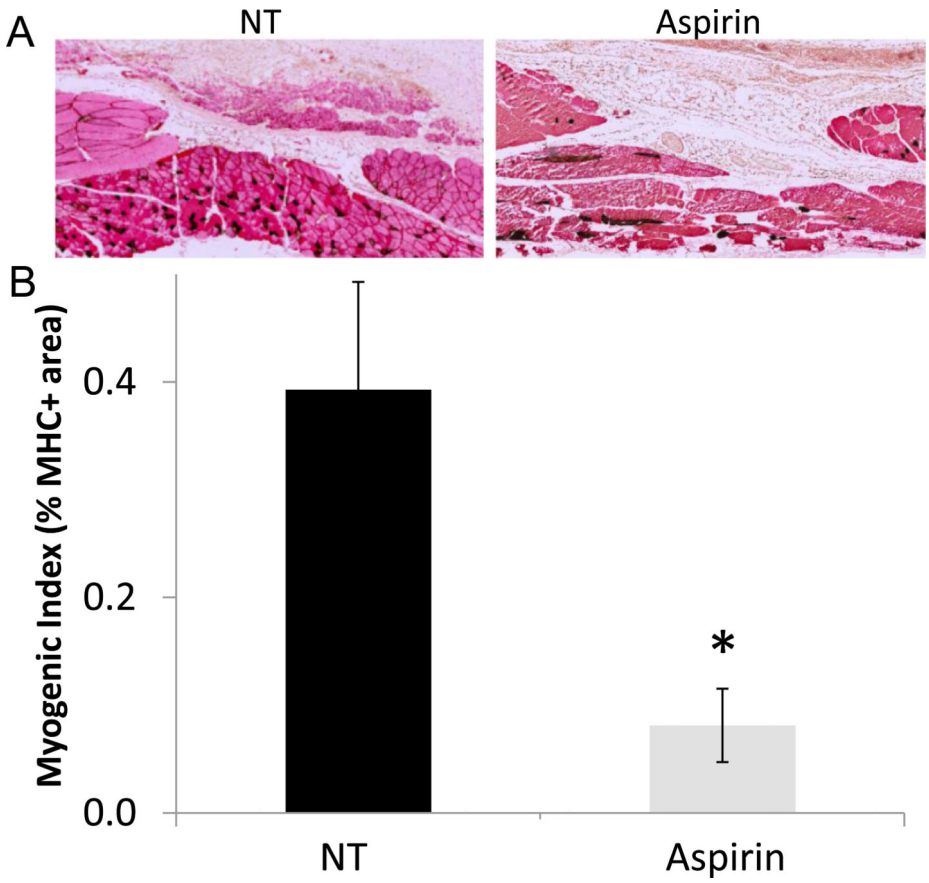

Figure 2.

The effect of aspirin administration on UBM stimulated myogenesis *in vivo*. Tissue sections from the specified time points were MHC stained and imaged. (A) Represenative images of tissue sections from untreated and aspirin treated animals 35 days post operatively are shown. (B) The myogenic index (total cross sectional area of MHC+ cells within the defect expressed as a function of the total defect area) was quantified at 35 days for untreated and aspirin treated animals. Significant decreases in myogenesis are shown ($p<0.05$).

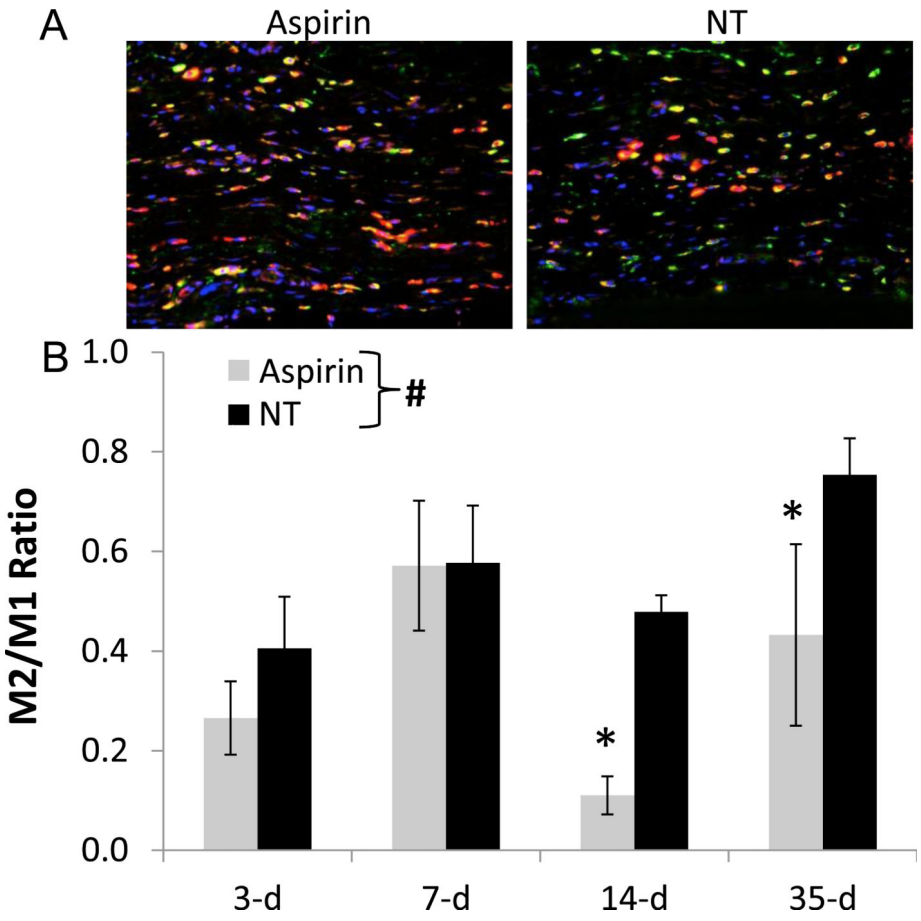

Figure 3.

The effect of aspirin administration on overall macrophage phenotype *in vivo* during UBM mediated constructive remodeling. Tissue sections from the specified time points were immunolabeled for CD68 (pan-macrophage, orange), CD206 (M2, green), and CD86 (M1, red) and imaged. Four representative images of each tissue section were collected and the number of CD68+CD206+ and CD68+CD86+ cells were quantified using Cell Profiler. (A) Representative images of tissue sections from untreated and aspirin treated animals are shown. (B) The mean M2/M1 ratio in the tissue sections is expressed as a ratio of CD68+CD206+ cells to CD68+CD86+ cells. #, a significant main effect (averaged data over all time points) for the untreated vs. aspirin treated groups is shown ($p<0.05$). *, significant differences in M2/M1 ratio ($p<0.05$) are shown.

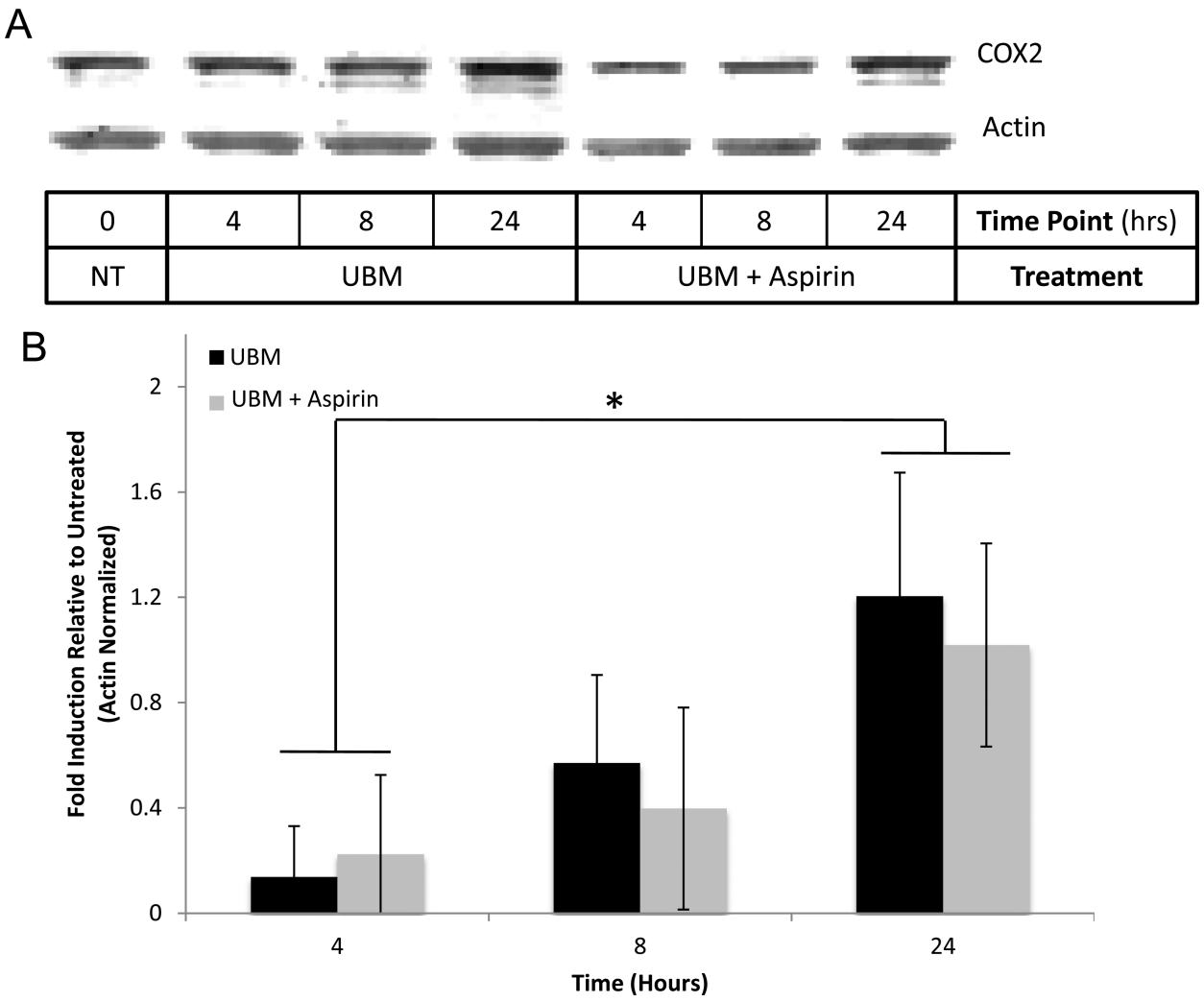

Figure 4.

The effect of UBM on COX2 expression and PGE2 secretion in THP1 cells. THP1 monocytes were differentiated to a macrophage-like cell lineage with PMA for 24 hours and rested for an additional 24 hours, after which, cells were stimulated with UBM hydrogel (0.5 mg/mL). Cell lysates were collected at 4, 8, and 24 hours, resolved on SDS PAGE gels , and immunoblotted for COX2 expression. Untreated cells collected at the 0 hour time point served as an expression control and actin was utilized as a loading control. (A) Representative immunoblots for aspirin treated and untreated cells are shown. (B) Relative changes in COX2 expression were determined using densitometry. The average change in COX2 expression is shown. Significant differences in COX2 expression ($p<0.05$) are shown.

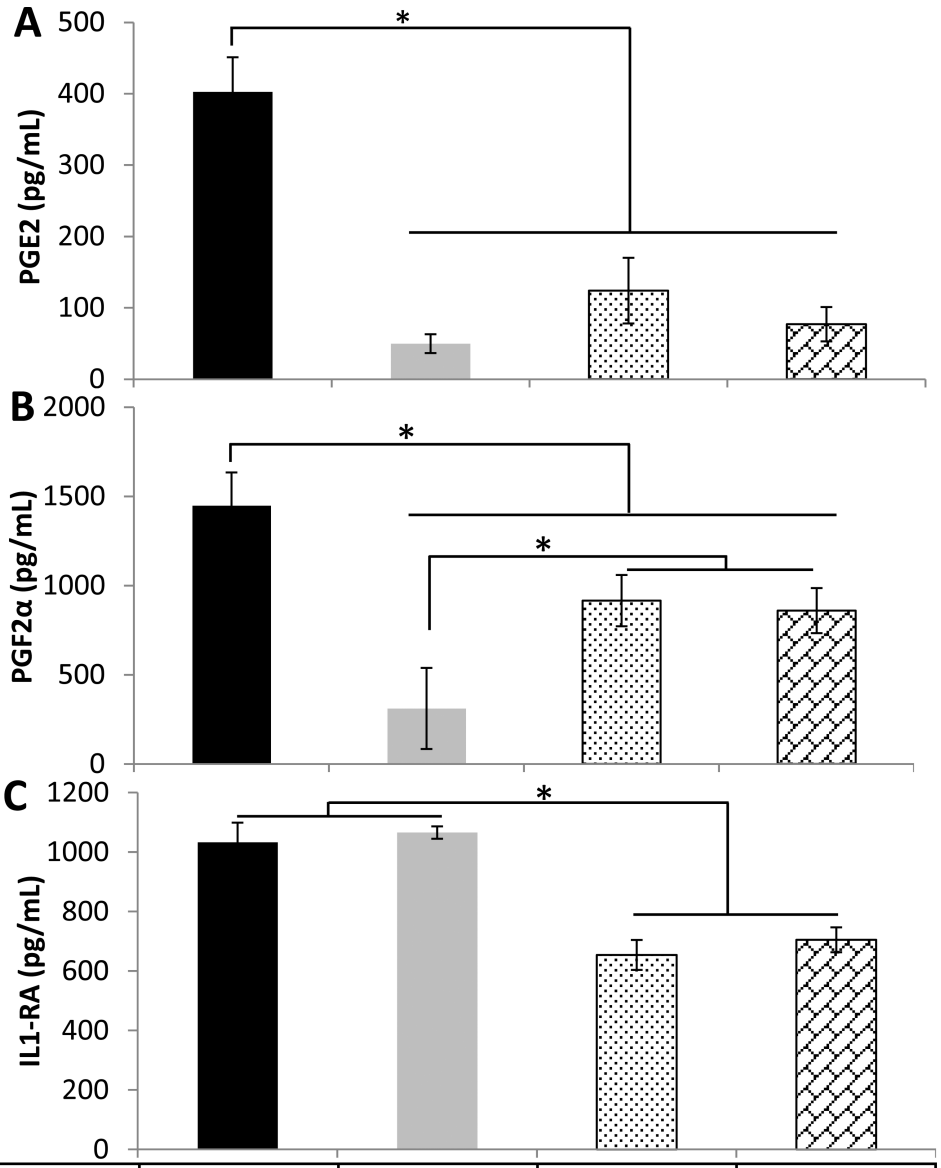

Treatment	UBM (0.5 mg/mL)	UBM (0.5 mg/mL)	Pepsin	No Treatment
Inhibitor	--	Aspirin (200 μM)	--	--

Figure 5.

The effect of Aspirin on PGE2, PGF2α, and IL-1RA production in UBM hydrogel treated macrophages *in vitro*. THP1 monocytes were differentiated to a macrophage-like cell lineage with PMA for 24 hours and rested for an additional 24 hours. Aspirin (200 μM) was added to cells for 1 hour prior to UBM hydrogel (0.5 mg/mL) addition. Cells were incubated for 48 hours and culture supernatants were collected. (A) PGE2, (B) PGF2α, and (C) IL-1RA concentrations in the culture supernatants were determined using commercially

available ELISA kits. Significant differences in secreted factor concentration are shown ($p<0.05$).

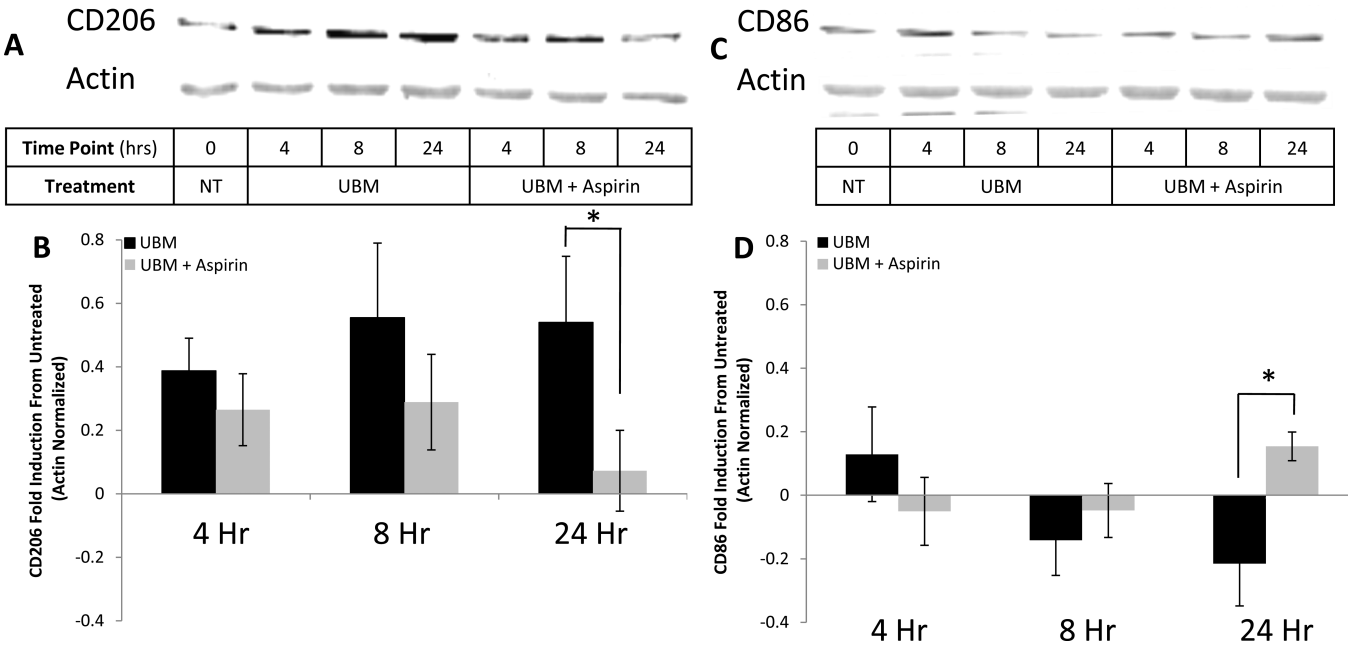

Figure 6.

The effect of aspirin treatment on CD206 and CD86 expression in macrophages treated with UBM hydrogel *in vitro*. THP1 monocytes were differentiated to a macrophage-like cell lineage with PMA for 24 hours and rested for an additional 24 hours. Aspirin (200 μM) was added to cells for 1 hour prior to UBM hydrogel (0.5 mg/mL) addition. Cell lysates were collected at 4, 8, and 24 hours, resolved on SDS gels, transferred to membranes, and immunoblotted for CD206 and CD86 expression. Actin served as a loading control. (A) Representative blot of CD206 expression and (B) relative changes in CD206 expression compared to 0 hr control measured with densitometry. (C) Representative blot of CD86 expression and (D) relative changes in CD86 expression compared to 0 hr control measured with densitometry. Significant differences in CD206 and CD86 expression between aspirin treated and untreated cells are shown ($p<0.05$).

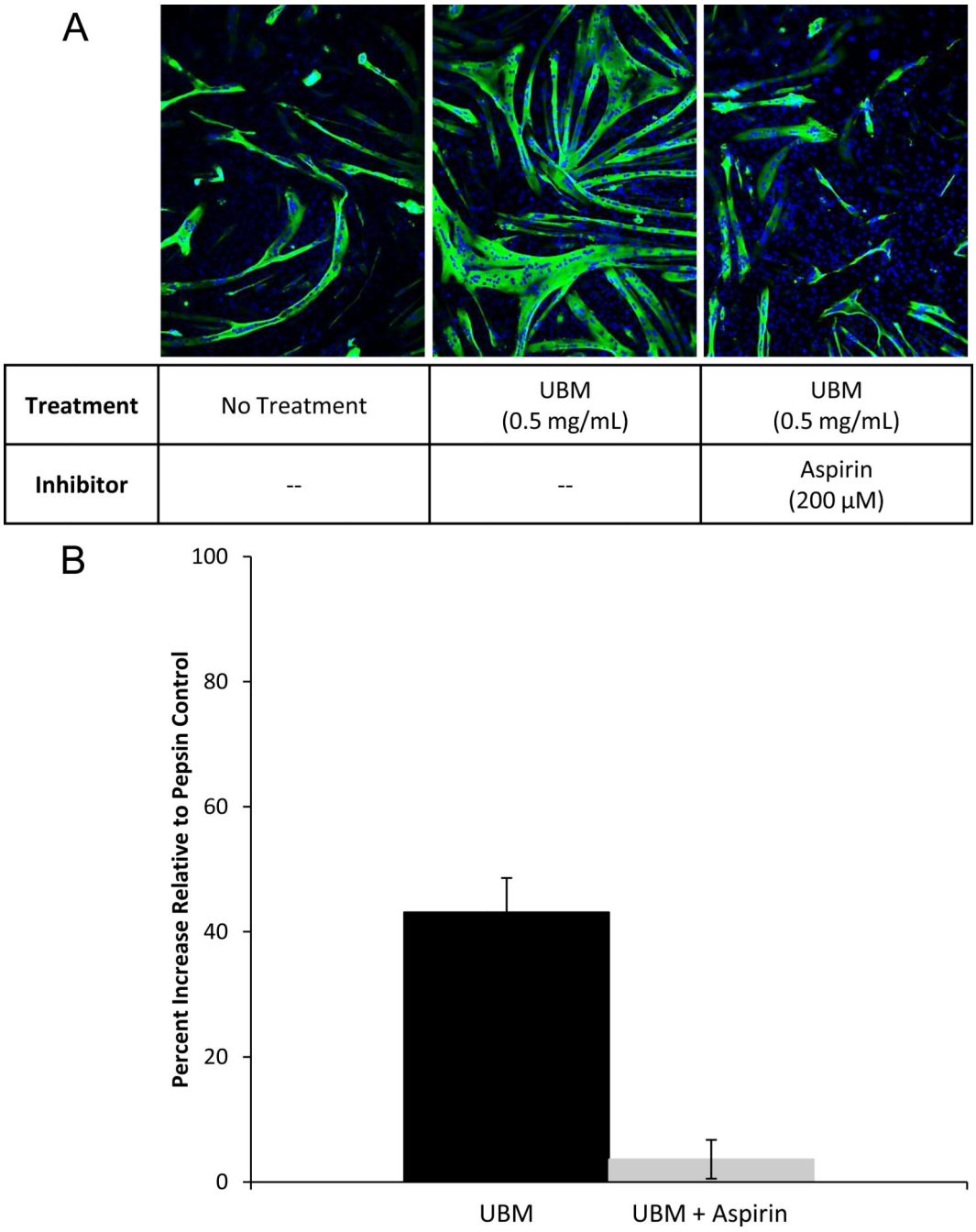

Figure 7.

The effect of aspirin treatment on myotube formation in UBM hydrogel treated co culture system. THP1 monocytes were differentiated with PMA and rested in a transwell insert. (A) Representative images of C2C12 myoblast fusion into MHC+ myotubes (green) stimulated with UBM and inhibited with Aspirin. Nuclei are stained with DAPI (blue). (B) The fusion index was calculated using quantitative image analysis of several indices of myogenesis. All data are expressed as a percentage change from digestion enzyme only control.